Regeneration of Activated Carbons Used in Waste-Water Treatment by a Moving-Bed Regenerator

A method was developed for calculating the distributions of weight loss and temperature of spent activated carbon in a moving-bed regenerator in which the solid flow was regarded as being plug flow. A kinetic model developed earlier, which was based on regeneration consisting of many first-order reactions each with different frequency factors and different activation energies, was successfully applied to a design method for the regenerator. The flow pattern of the solid particles and heat transfer characteristics in a small moving bed were clarified experimentally, and the information obtained was used to calculate the distributions of weight loss of the spent carbon and temperature in the moving-bed regenerator by means of the design method. The calculated results were in fairly good agreement with the experimental data obtained in a small moving-bed regenerator. The adsorption capacity of the regenerated carbon was comparable to or greater than that of the virgin carbon.

KENJI HASHIMOTO, KOUICHI MIURA and SUSUMU KYOTANI

Department of Chemical Engineering
Kyoto University
Kyoto, 606, Japan

SCOPE

Activated carbon has been used in many adsorption processes for removal of toxic substances, recovery of valuable substances, separation of mixtures, and so on. Recently, the use of activated carbon in advanced waste-water treatment has attracted attention. For this treatment to be economical, the spent activated carbon must be repeatedly regenerated and reused.

The granular activated carbon used in waste-water treatment can be regenerated thermally in a steam atmosphere. The regenerator used is usually a moving-bed reactor, which provides uniform regeneration and minimizes the loss due to abrasion. The spent carbon fed into the regenerator is heated from room temperature to almost 1,000°C. During the heating process the spent carbon is regenerated through such reactions as thermal desorption and pyrolysis of the adsorbates, and gasification of the carbonized adsorbates and the activated carbon itself. To design such a moving-bed regenerator, the kinetics of the thermal regeneration reactions and the heat transfer characteristics and flow pattern of the solid particles in the regenerator must be investigated.

This paper aims to present a rational design method for a moving-bed regenerator in which solid particles descend in a plug flow, and to examine whether thermal regeneration in the moving bed effectively restores the adsorption capacity of the activated carbon.

CONCLUSIONS AND SIGNIFICANCE

A method was developed for calculating the distributions of temperature and weight loss of spent carbon in a moving-bed regenerator where the solid flow was assumed to be plug flow. The kinetics of thermal regeneration was represented by a distribution curve of the activation energy for pyrolysis and the rate constant for gasification obtained by measurement of thermogravimetric curves. The effective thermal conductivity and the wall heat transfer coefficient were measured for the same moving bed. The distributions of temperature and weight loss in the moving-bed regenerator were calculated by applying the method developed to the data obtained. The calculated distributions were in fairly good agreement with the experimental data, indicating that the method is valid for the practical design of a thermal regenerator for activated carbon.

The adsorption capacity of the regenerated carbon was comparable to or greater than that of the virgin carbon. This indicated that the activated carbon used in waste-water treatment was efficiently regenerated with steam in the moving-bed reactor.

INTRODUCTION

In recent years granular activated carbon has been widely used for advanced waste-water treatment. Because it is expensive, activated carbon must be repeatedly regenerated and reused. Of several regeneration methods, thermal regeneration in a steam atmosphere is now the most effective for regenerating the activated carbon used in waste-water treatment.

Several types of regenerators, such as the rotary kiln, the multiple furnace, the moving bed, and the fluidized bed, have been tested. The moving-bed type has been found to regenerate the spent carbon uniformly and to minimize the loss of carbon caused by abrasion. The spent carbon fed into these regenerators is heated gradually from room temperature to about 1,000°C. The thermal regeneration processes in these regenerators consists of a series of steps: drying (up to 100°C), thermal desorption (110 to 250°C), pyrolysis and carbonization (200 to 650°C), and gasification in the high temperature region (650 to 1,000°C). To design such regenerators rationally, the kinetics of the thermal regeneration and the heat transfer characteristics and flow pattern of the solid particles in the regenerators should be known. In a previous paper (Hashimoto et al., 1982) we analyzed thermal regeneration based on the assumption that it involves many first-order reactions each with a different activation energy and frequency factor.

In this work the kinetics of thermal regeneration was analyzed by extending our previously developed model. The flow pattern of the solid particles was ascertained experimentally to be plug flow. The effective thermal conductivity and the wall heat transfer coefficient in a small moving bed were measured. These data were used to calculate the distributions of temperature and weight loss of the spent carbon in the small moving-bed regenerator, and the predictions were compared with the experimental data obtained in the same regenerator. Finally, the physical properties and the adsorption characteristics of the regenerated carbon were measured to examine whether the regeneration in the moving-bed reactor was effective.

THE KINETICS OF REGENERATION

The thermal regeneration of spent carbon in a steam atmosphere involves pyrolysis of the adsorbed substances to yield volatile matter and carbonized adsorbates, and the simultaneous gasification of both the carbonized adsorbates and the activated carbon itself. Previously, the authors have analyzed thermal regeneration involving both pyrolysis and gasification by introducing a distribution function of the activation energy (Hashimoto et al., 1982). This method was successfully used to predict the weight change of activated carbon during thermal regeneration in a thermobalance reactor. For designing a moving-bed regenerator, however, the rates of pyrolysis and gasification must be known separately, because the temperature distribution in the moving bed is affected by the heats of reaction, which are different for the two reactions. To formulate separately the rates of pyrolysis and gasification, two additional assumptions were introduced into the earlier model:

1. The gasification rate of the carbonized adsorbate is equal to that of the activated carbon.
2. The rate of weight change of the sample caused by the gasification is proportional to the weight of the sample.

The activated carbon used in waste-water treatment usually adsorbs various kinds of organic substances. It is first assumed that the jth adsorbate is pyrolyzed to volatile matter and a carbonized adsorbate. Then the carbonized adsorbate and the active carbon react with steam and are gasified. It is further assumed that the carbonized adsorbate and the activated carbon give the same gaseous products. The following reaction stoichiometries can then be formulated.

Pyrolysis:

$$\underset{(j\text{th adsorbate})}{Q_j} \rightarrow \underset{(\text{volatile matter})}{\phi_j V_j} + \underset{(\text{carbonized adsorbate})}{\psi_j S_j} \tag{1}$$

Gasification of the carbonized adsorbate and the active carbon:

$$S_j \rightarrow gG \tag{2}$$

$$\underset{(\text{active carbon})}{C} \rightarrow \underset{(\text{gaseous products})}{gG} \tag{3}$$

The reaction between the carbonaceous material and steam is often represented by first-order kinetics. In this case, the weight change of each species is represented by

$$\frac{dq_j}{dt} = -k_{0j} q_j e^{-E_j/RT} \tag{4}$$

$$\frac{dv_j}{dt} = \frac{v_j^*}{q_{j0}}\left(-\frac{dq_j}{dt}\right) \tag{5}$$

$$\frac{ds_j}{dt} = \frac{s_j^*}{q_{j0}}\left(-\frac{dq_j}{dt}\right) - k_{0g} e^{-E_g/RT} s_j \tag{6}$$

where the subscript j represents the jth adsorbed substance; the subscript g represents gasification; q_j, v_j, and s_j represent respectively the weights of Q_j, V_j, and S_j per initial unit weight of the active carbon; s_j^* and v_j^* represent respectively the s_j and v_j values at the completion of Reaction 1 in an inert atmosphere; k_0 is the frequency factor; E is the activation energy.

Integrating Eq. 4 with the initial condition $q_j = q_{j0}$ at $t = 0$ gives

$$q_j = q_{j0} \exp\left(-k_{0j} \int_0^t e^{-E_j/RT} dt\right) \tag{7}$$

Equation 4 is rewritten by use of Eq. 7 as

$$\frac{dq_j}{dt} = -k_{0j} e^{-E_j/RT} q_{j0} \exp\left(-k_{0j} \int_0^t e^{-E_j/RT} dt\right) \tag{8}$$

The activation energy and frequency factor for pyrolysis differ for each of the adsorbed substances. The fraction of adsorbates whose activation energy for pyrolysis lies between E_j and $E_j + \Delta E$ is represented by $f(E_j)\Delta E$, namely,

$$q_{j0} = q_0 f(E_j)\Delta E \tag{9}$$

$$\int_0^\infty f(E)dE = 1 \tag{10}$$

By inserting Eq. 9 into Eqs. 7 and 8 and summing up the equations for all species, the following equations are obtained.

$$q = \sum q_j = q_0 \int_0^\infty \exp\left(-k_0 \int_0^t e^{-E/RT} dt\right) f(E)dE \tag{11}$$

$$\frac{dq}{dt} = \sum\left(\frac{dq_j}{dt}\right) = -q_0 \int_0^\infty k_0 e^{-E/RT} \times \exp\left(-k_0 \int_0^t e^{-E/RT} dt\right) f(E)dE \tag{12}$$

The frequency factor k_0 was correlated approximately by (Hashimoto et al., 1982)

$$k_0 = \alpha \exp(\beta E),\ \alpha = 1{,}000\ \text{s}^{-1},\ \beta = 0.043\ \text{mol/kJ} \tag{13}$$

By assuming that the ratio v_j^*/s_j^* is constant ($= v^*/s^*$) irrespective of the species, Eqs. 5 and 6 can be summed up directly for all species to give

$$\frac{dv}{dt} = \sum\left(\frac{dv_j}{dt}\right) = \frac{v^*}{q_0}\left(-\frac{dq}{dt}\right) \tag{14}$$

$$\frac{ds}{dt} = \sum\left(\frac{ds_j}{dt}\right) = \frac{s^*}{q_0}\left(-\frac{dq}{dt}\right) - k_{0g}se^{-E_g/RT} \tag{15}$$

Here it is assumed that $q_0 = s^* + v^*$ based on the stoichiometry of Eq. 1.

Equation 14 is readily integrated to give

$$v = \sum v_j = \frac{v^*}{q_0}(q_0 - q) \tag{16}$$

Since Eq. 15 is a differential equation of the type of $dy/dx + Q(x)y = P(x)$, it can be integrated as

$$s = \sum s_j$$

$$= \frac{s^*}{q_0}\exp\left(-k_{0g}\int_0^t e^{-E_g/RT}dt\right)\int_0^t\left[\left(-\frac{dq}{dt}\right)\right.$$

$$\left.\times \exp\left(k_{0g}\int_0^t e^{-E_g/RT}dt\right)\right]dt \tag{17}$$

Thus the weight changes in the adsorbed substances were formulated by Eqs. 11, 16, and 17.

Activated carbon itself is also gasified by oxidant, and the change in the active carbon weight W_A was represented by first-order kinetics as

$$\frac{dW_A}{dt} = -k_{og}W_Ae^{-E_g/RT} \tag{18}$$

$$W_A = W_{A0}\exp\left(-k_{0g}\int_0^t e^{-E_g/RT}dt\right) \tag{19}$$

The total weight of the sample of W_T is obtained from the definitions of q, s, and v as follows:

$$W_T = W_A + W_{A0}(q + s) \tag{20}$$

The change in W_T is also given by use of Eqs. 14, 15, and 20 as

$$\frac{dW_T}{dt} = W_{A0}\frac{v^*}{q_0}\left(\frac{dq}{dt}\right) - k_{0g}e^{-E_g/RT}(W_A + W_{A0}s) \tag{21}$$

Dividing both sides of Eq. 21 by $(-W_T)$ gives

$$-\frac{1}{W_T}\frac{dW_T}{dt} = \frac{W_{A0}}{W_T}\frac{v^*}{q_0}\left(-\frac{dq}{dt}\right)$$

$$+\frac{1}{W_T}k_{0g}e^{-E_g/RT}(W_A + W_{A0}s) \tag{22a}$$

The lefthand side of Eq. 22a represents the apparent rate of decrease of total solid materials, and is designated by $-r_T$. The first term on the righthand side corresponds to the overall rate of pyrolysis; the second term represents the gasification rate of both carbonized adsorbates and activated carbon. Then Eq. 22a is simply represented in terms of these reaction rates as

$$-r_T = \frac{v^*}{q_0}r_P + r_G \tag{22b}$$

where

$$r_T = \frac{1}{W_T}\left(\frac{dW_T}{dt}\right) \tag{23}$$

$$r_P = \frac{W_{A0}}{W_T}\left(-\frac{dq}{dt}\right) \tag{24}$$

$$r_G = \frac{1}{W_T}k_{0g}e^{-E_g/RT}(W_A + W_{A0}s) \tag{25}$$

Thus the rates of pyrolysis and gasification were separated. Equations 11 to 25 indicate that r_P and r_G can be represented as functions of t, T and W_T when $f(E)$ is determined and the ratio v^*/s^* is known. The distribution curve $f(E)$ can be obtained by analyzing the thermogravimetric curve measured under a constant heating rate in an inert atmosphere. The detailed procedure to determine $f(E)$ was presented in our previous paper (Hashimoto et al., 1982).

DESIGN EQUATION FOR A MOVING-BED REGENERATOR

A cylindrical type of moving-bed regenerator as shown in Figure 1 was employed. The spent carbon particles fed to the top of the regenerator descend at a constant linear velocity u_s and come into contact with a countercurrent gas stream while being heated from the wall. The following assumptions were made in deriving the design equations:

1. The temperature difference between the solid and the gas is negligibly small.
2. Both the solid and the gas flows are represented by the plug flow.
3. The effective radial thermal conductivity k_e and the wall heat transfer coefficient h_w are constant.
4. The amount of gas evolved by the regeneration reaction is negligible. Therefore the steam pressure in the regenerator remains constant.

With these assumptions the basic equations for a steady state were derived.

The mass balance equations for the solid and the residual amount adsorbed q can be represented by use of Eqs. 22 and 25 as follows:

$$-\frac{\partial G_s}{\partial z} = \rho_b(-r_T) = \rho_b\left(\frac{v^*}{q_0}r_P + r_G\right) \tag{26}$$

$$G_{A0}\left(-\frac{\partial q}{\partial z}\right) = -\frac{G_{s0}}{1 + q_0}\left(\frac{\partial q}{\partial z}\right) = \rho_b r_P \tag{27}$$

where G_s is the mass velocity of the solid, subscript b is the packed density and G_{A0} is the mass velocity of the activated carbon at the inlet of the regenerator.

The overall heat balance is given by

$$-\frac{\partial(G\bar{c}_pT)}{\partial z} + k_e\left(\frac{\partial^2 T}{\partial r^2} + \frac{1}{r}\frac{\partial T}{\partial r}\right)$$

$$+\rho_b\left[\frac{v^*}{q_0}r_P(-\Delta H_P) + r_G(-\Delta H_G)\right] = 0 \tag{28}$$

where ΔH_P and ΔH_G represent respectively the heat of the pyrolysis reaction to form 1 kg of volatile matter and that of the gasification reaction per 1 kg of carbon gasified. The term $G\bar{c}_p$ represents

$$G\bar{c}_p = G_sc_{ps} - G_g\bar{c}_{pg} \tag{29}$$

where c_{ps} is the specific heat of the solid, $\bar{c}_{pg}$ is the averaged

TABLE 1. PHYSICAL PROPERTIES OF SPENT ACTIVE CARBON

Bulk Density of Bed ρ_b kg/m³	Particle Density ρ_p kg/m³	Particle Diameter d_p m	Pore Surface Area S_{BET} m²/kg
465	751	1.45×10^{-3}	6.38×10^5

specific heat of the gas mixture, and G_g is the mass velocity of the gas.

The boundary conditions for the above equations are given as follows:

$$T = T_0(r),\ G_s = G_{s0} \text{ at } z = 0 \tag{30}$$

$$-k_e \frac{\partial T}{\partial r} = h_w(T - T_w)$$

$$= \frac{\lambda}{R_1}(T_w - T_s)/\ln(R_2/R_1) \text{ at wall} \tag{31}$$

$$\frac{\partial T}{\partial r} = 0 \text{ at } r = 0 \tag{32}$$

$$T_s = T_s(z) \text{ for } 0 < z < L \tag{33}$$

where R_1 and R_2 are respectively the inner and the outer radii of the regenerator, T_w is the inside wall temperature, T_s is the outside wall temperature, and λ is the thermal conductivity in the wall of the regenerator.

The basic equations were converted to finite-difference equations by the Crank-Nicolson scheme and solved numerically (see Appendix). To solve the basic equations the rate of the thermal regeneration, namely, $f(E)$, k_{0g} and E_g, the effective thermal conductivity k_e, and the wall heat transfer coefficient h_w must be measured.

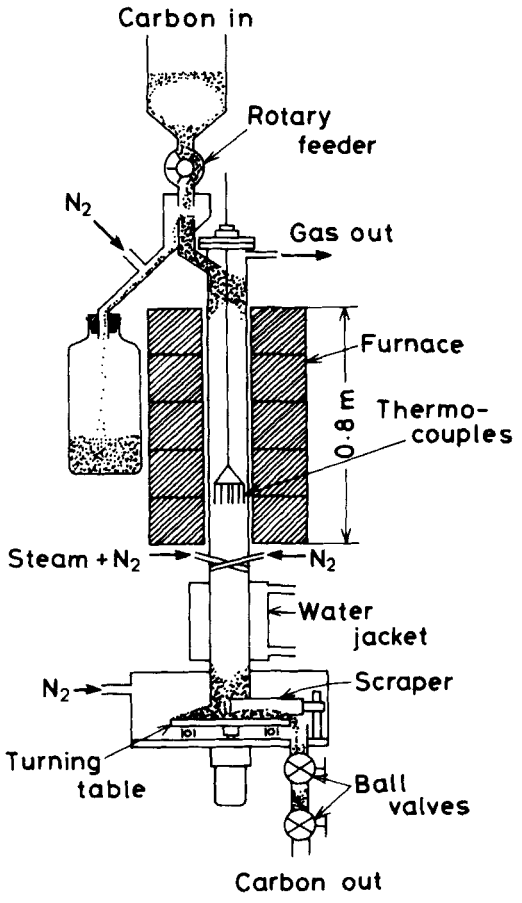

Figure 1. The moving-bed regenerator used.

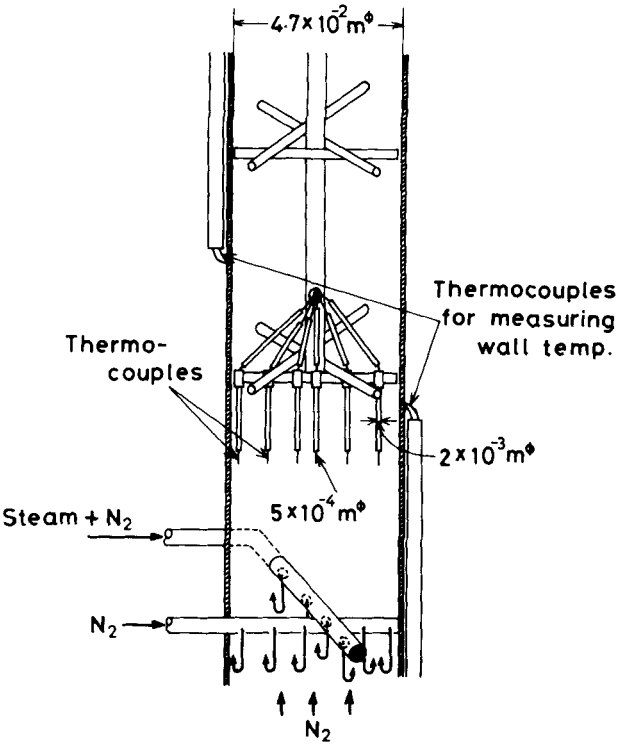

Figure 2. Details of the set of thermocouples and gas inlets.

EXPERIMENTAL

Spent Activated Carbon

Activated Carbon (Takeda, Japan) used in the waste-water treatment of a dye works was employed as a sample. The physical properties of the spent carbon are given in Table 1.

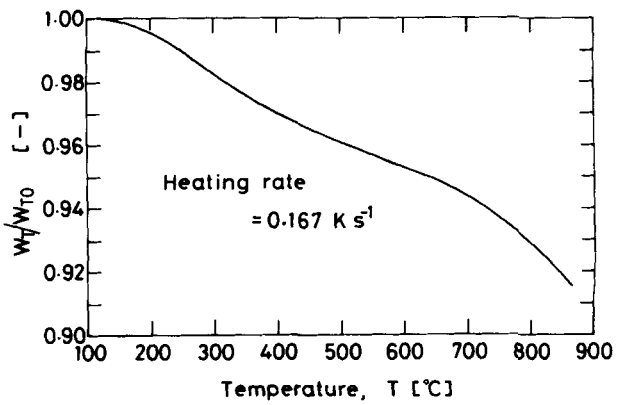

Figure 3. Thermogravimetric (TG) curve of the spent carbon measured in a nitrogen atmosphere.

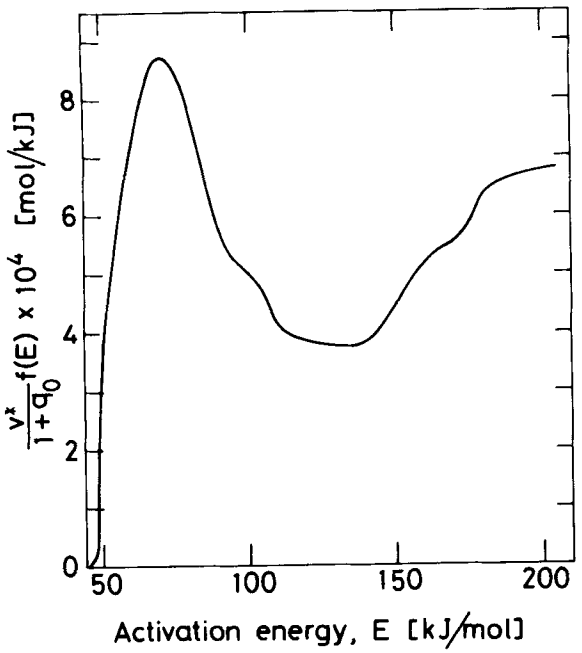

Figure 4. Distribution of activation energy for regeneration in a nitrogen atmosphere.

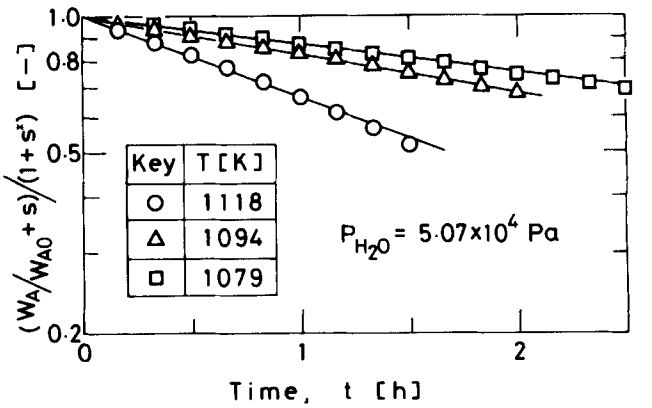

Figure 5. Gasification rates of carbonized adsorbates and active carbon

Determination of $f(E)$, k_{0g}, and E_g

A thermobalance reactor was used to measure the rate of thermal regeneration. To obtain the distribution curve of the activation energy $f(E)$ of pyrolysis, the thermogravimetric curve (TG curve) of the spent carbon was measured under a constant heating rate of 0.167 K/s in a nitrogen atmosphere.

To determine k_{0g} and E_g, a sample consisting of activated carbon and carbonized adsorbate, which was prepared by heating spent carbon to 1,123 K in a nitrogen atmosphere, was gasified with steam in the thermobalance at several constant temperatures between 1,048 and 1,118 K.

Measurement of Solid Particle Flow Pattern

To check if the solid particles descend in a plug flow, the flow pattern of the solid particles was measured at room temperature. A moving-bed apparatus made of transparent acrylic resin was used for this measurement. The moving bed was 1.00 m long and could be dismantled into four sections of lengths 0.40, 0.20, 0.20, and 0.20 m by unfastening the flanges. Particles of an activated carbon (Calgon Co.) were continuously fed to the top of the moving bed and discharged onto a turning table at the bottom. After a steady-state flow was attained, thin layers of tracer particles of silica alumina were added at the top of the moving bed. When these tracer particles reached the middle of one of the sections of the moving bed, the turntable was stopped and the section was removed carefully. A hot aqueous solution of agar-agar was poured into the section. After cooling the section in a water bath, the coagulated mass of particles was withdrawn and sliced vertically to observe the state of the tracer particles.

Measurement of k_e and h_w

Figure 1 shows a schematic representation of the apparatus used for measuring k_e and h_w as well as for regenerating the spent carbon.

The reactor (moving bed) was made of stainless steel tube 1.20 m long and 4.7×10^{-2} m I.D. The reactor was heated by an electric furnace of 0.80 m long. The furnace was divided into five equal sections, each of which was connected to a temperature controller, which allowed the longitudinal temperature distribution of the reactor wall to be changed.

Particles were fed to the top of the moving bed by means of a rotary feeder. The level of particles was kept constant by maintaining an overflow of particles. The descending particles were discharged from the reactor onto the turntable and, intermittently, to the surroundings by opening the two ball valves. Nitrogen and steam were fed to three inlets in the lower part of the moving bed.

The wall temperatures at different axial positions were measured with 11 thermocouples embedded in the reactor wall. Five of these were each connected to a temperature controller. The radial temperature distribution at an arbitrary axial position was measured with a set of six thermocouples arranged in the shape of a fish spear, which was movable vertically. Figure 2 shows the details of the set of thermocouples and the gas inlets.

The radial effective thermal conductivity k_e and the wall heat transfer coefficient h_w were measured at a constant wall temperature of about 673 K. Because it was impossible to keep the wall temperature constant over the whole length of the reactor, a section 0.2 to 0.3 m in length located in the middle of the furnace was employed for the measurement, during which time its wall temperature was kept constant.

Regeneration of Spent Activated Carbon

In commercial moving-bed regenerators the wall temperature usually varies in the axial direction. To realize this situation in the experimental reactor, the wall temperature was controlled such that it varied from room temperature at the top of the reactor to about 1,120 K in the middle, in line with the temperature distribution in a commercial regenerator (Loven, 1973).

The temperature distribution throughout the reactor was measured as follows: The set of thermocouples was first lowered to the lower part of the reactor and the radial temperatures were measured after the steady state was attained, normally after 3 to 4 h. Then the thermocouples were raised by about 0.04 to 0.05 m, and the temperatures were measured again after 10 min. This procedure was repeated until the thermocouples reached the top of the reactor. Thus the radial and the axial temperature distributions throughout the reactor were measured.

The packed density ρ_b, the particle density ρ_p, the true density ρ_t, the particle diameter d_p, the pore surface area S_{BET}, and the pore volume distribution of the regenerated carbon were measured. The adsorption isotherm of aqueous p-nitrophenol solution on the regenerated carbon was also measured to evaluate the degree of regeneration.

RESULTS AND DISCUSSION

Rate of Thermal Regeneration

Figure 3 shows the thermogravimetric (TG) curve of the spent activated carbon measured in a nitrogen atmosphere at the heating rate of 0.167 K/s. From this TG curve the distribution curve of the activation energy $f(E)$ for pyrolysis was obtained, as shown in Figure 4. The distribution curve $f(E)$ covers the range of E = 50 to 200 kJ/mol. This indicates that various substances were adsorbed on the spent activated carbon.

Gasification rates were measured at the steam pressure, P_{H_2O}, of 5.07×10^4 and 2.79×10^4 Pa. Figure 5 shows the changes in the

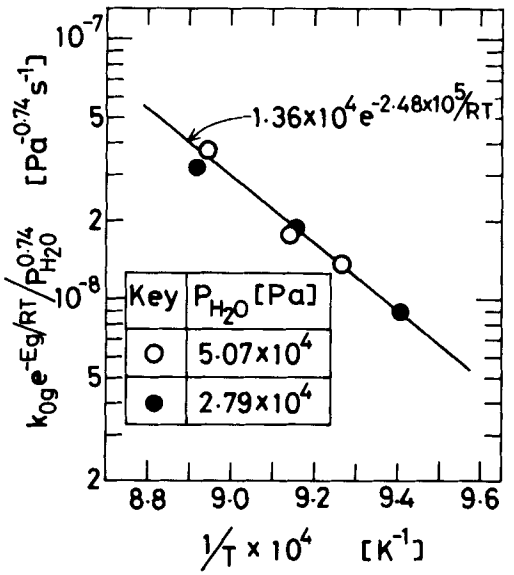

Figure 6. Arrhenius plot of the gasification rate constants.

relative weight of the activated carbon and carbonized adsorbates owing to gasification at temperatures of 1,079, 1,094, and 1,118 K. It reveals that the rate of weight decrease is proportional to the weight of the sample, which supports the assumption made in developing the rate equation.

To derive the design equation, the steam pressure in the moving bed was assumed to be constant, as stated earlier. This means that k_{0g} is constant under given experimental conditions. To apply the design equation to a wide range of experimental conditions, however, the dependency of k_{0g} on steam pressure, P_{H_2O}, should be formulated. The method of least squares was used to derive the following equation, although k_{0g} was measured only at two different steam pressures.

$$k_{0g} = 1.36 \times 10^4 (P_{H_2O})^{0.74} [s^{-1}] \quad (34)$$

The activation energy E_g was obtained simultaneously by the method of least squares as

$$E_g = 2.48 \times 10^5 [J/mol] \quad (35)$$

Figure 6 shows an Arrhenius plot of the experimental data and the line calculated by use of k_{0g} and E_g thus obtained. It is evident that this steam pressure dependency of k_{0g} and the value of E_g are reasonable.

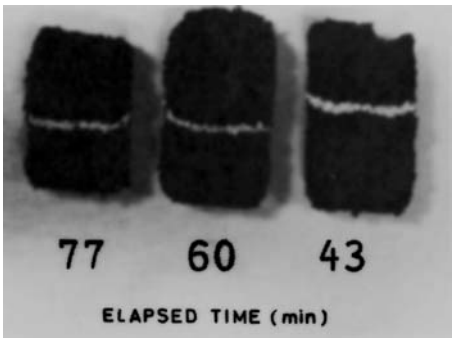

Figure 7. Tracer particles within the moving bed of carbon particles at different residence times.

TABLE 2. EXPERIMENTAL CONDITIONS AND RESULTS OF HEAT TRANSFER EXPERIMENTS

Run	P_{H2O} Pa	G_g kg/m²·h	G_s kg/m²·h	T_w K	k_e W/m·K	h_w W/m²·K
H1	5.07×10^4	107	536	674	0.297	49.4
H2	5.07×10^4	92.2	598	678	0.195	63.1
H4	2.79×10^4	156	528	677	0.169	28.6

Flow Pattern of Solid Particles

Figure 7 is a photograph of the tracer particles within the carbon particles at three different residence times. The tracer particles hardly diffuse from the flat layers formed at the top of the moving bed. This indicates that the assumption of the plug flow is valid for the particles in the regenerator.

Effective Radial Thermal Conductivity k_e and Wall Heat Transfer Coefficient h_w

Based on similar assumptions to those employed for developing the design equations, an equation representing the temperature distributions in a moving bed which is heated from the wall of constant temperature T_w is given elsewhere (Carslaw and Jaeger, 1959) as follows:

$$T - T_w = 2 \sum_{n=1}^{\infty} e^{-\kappa\alpha_n^2 x} \frac{\alpha_n^2 J_0(\alpha_{ny})}{(h^2 + \alpha_n^2)[J_0(\alpha_n)]^2} \times \int_0^1 y[T_0(y) - T_w] J_0(\alpha_n y) dy \quad (36)$$

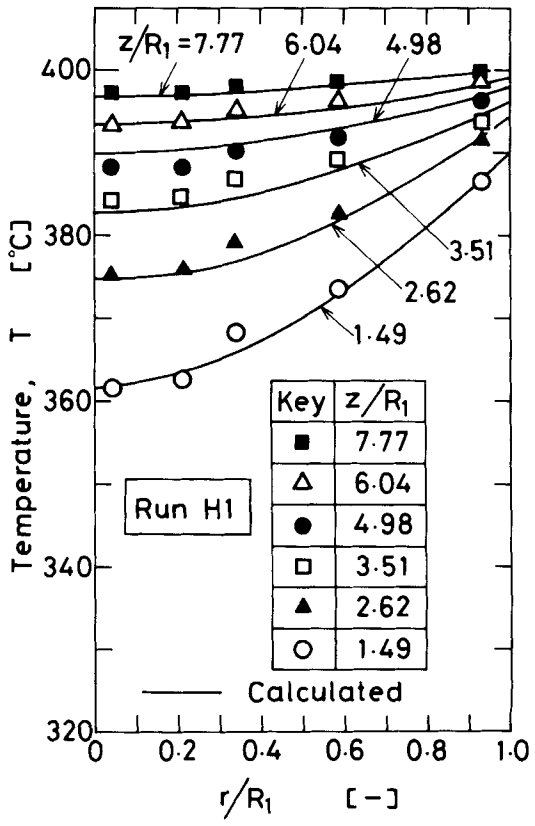

Figure 8. Temperature distributions calculated by use of k_e and h_w, and experimental data (run H1).

TABLE 3. EXPERIMENTAL CONDITIONS FOR THERMAL REGENERATION

Run	P_{H2O} Pa	G_g kg/m²·h	G_s0 kg/m²·h
1	5.07×10^4	107	536
2	5.07×10^4	92.2	598
3	5.07×10^4	107	536
4	2.79×10^4	156	528

where J_0 and J_1 represent the Bessel functions of the 0th and first orders, respectively. The dimensionless parameters including k_e and h_w are defined by

$$\kappa = k_e/(G_s c_{ps} - G_g \bar{c}_{pg}) \tag{37}$$

$$h = h_w R_1/k_e \tag{38}$$

The dimensionless axial length x and radial position y are defined as $x = z/R_1$ and $y = r/R_1$, respectively. $T_0(y)$ represents the temperature distribution at the solid inlet ($z = 0$), and α_n is the nth positive root of the following transcendental equation

$$\alpha_n J_1(\alpha_n) = h J_0(\alpha_n) \tag{39}$$

When $\kappa x > 0.2$, the infinite series in Eq. 36 is approximated by the first term, and Eq. 36 reduces to

$$T - T_w = 2Ke^{-\kappa\alpha_1^2 x}\left\{\frac{\alpha_1 J_1(\alpha_1) J_0(\alpha_1 y)}{(h^2 + \alpha_1^2)[J_0(\alpha_1)]^2}\right\} \tag{40}$$

where

$$K = \frac{\alpha_1}{J_1(\alpha_1)} \int_0^1 y[T_0(y) - T_w] J_0(\alpha_1 y) dy \tag{41}$$

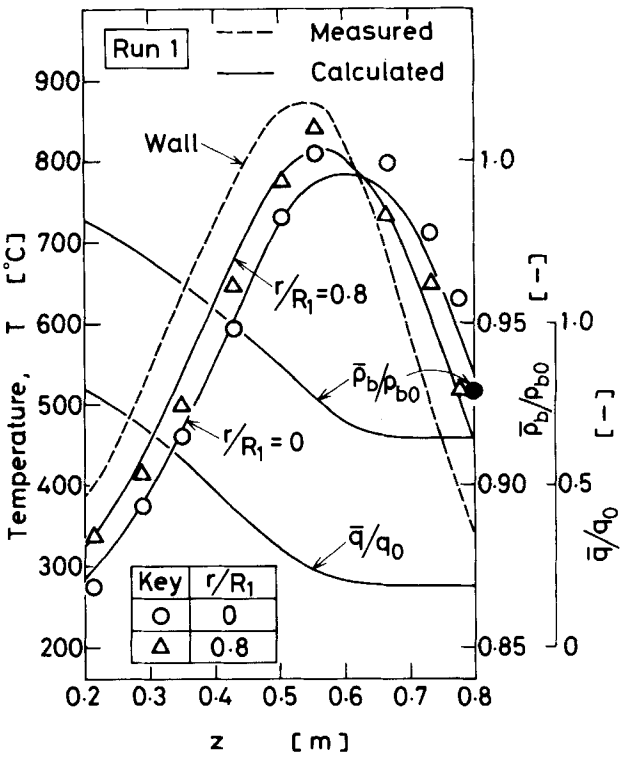

Figure 9b. Predicted axial distributions of T, $\bar{p}_b$, and $\bar{q}$, and experimental data (run 1)

The values of k_e and h_w were determined so that the temperature distributions calculated by Eqs. 40 and 41 might fit those obtained experimentally. The heat capacity of the activated car-

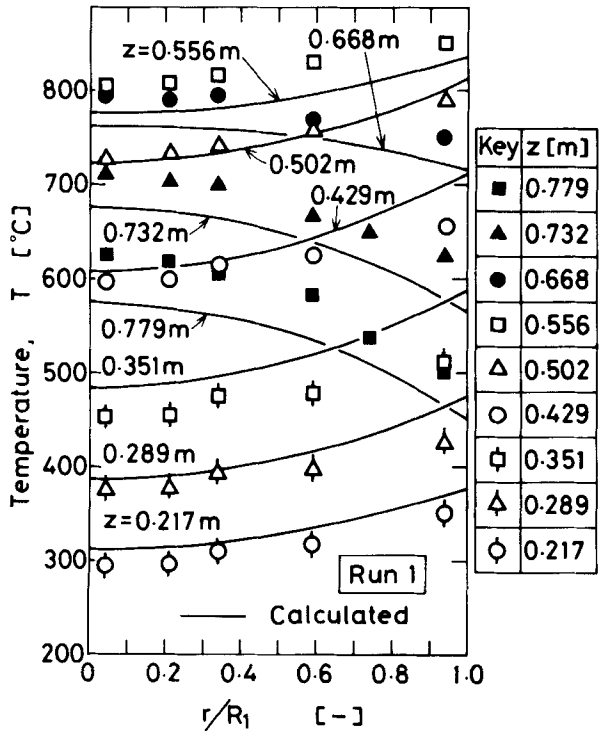

Figure 9a. Predicted radial distributions of temperature and experimental data (run 1)

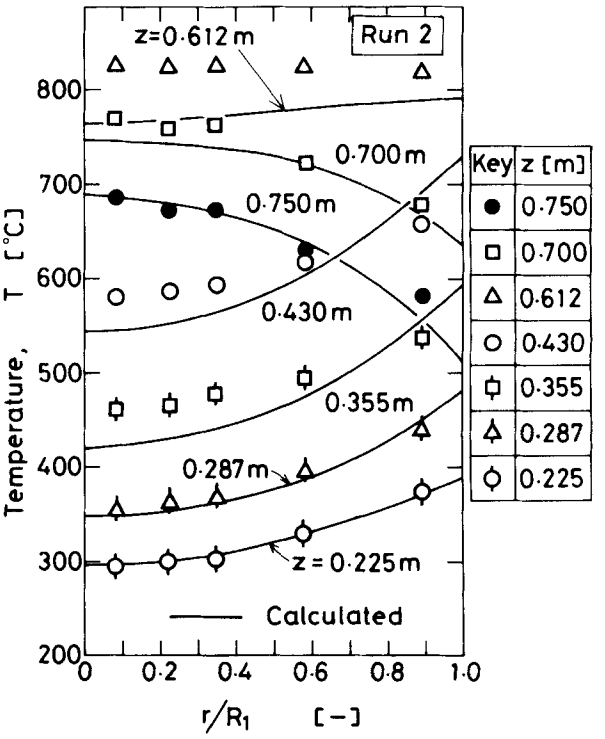

Figure 10a. Predicted radial distributions of temperature and experimental data (run 2).

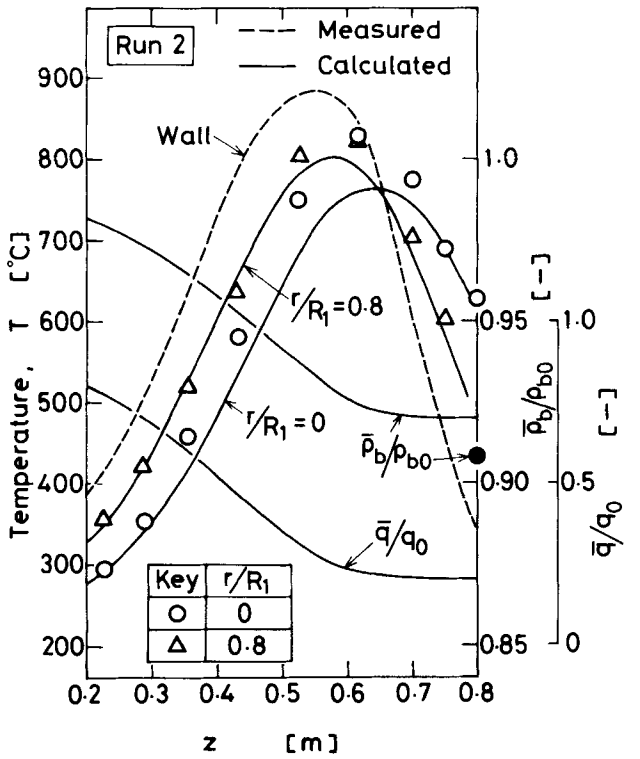

Figure 10b. Predicted axial distributions of T, $\bar{\rho}_b$, and $\bar{q}$, and experimental data (run 2).

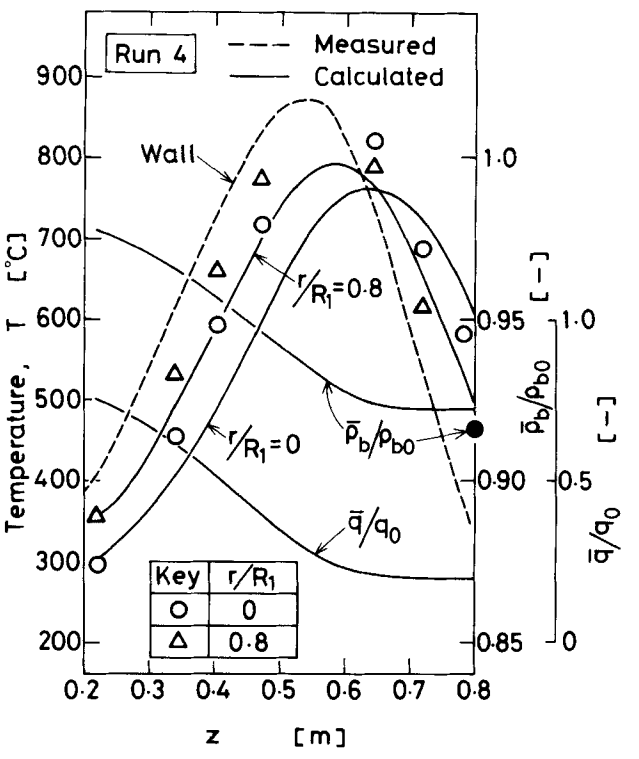

Figure 12. Predicted axial distributions of T, $\bar{\rho}_b$, and $\bar{q}$, and experimental data (run 4).

bon c_s was set at 1.2 kJ/kg·K for the simulation. The experimental conditions and the determined k_e and h_w values are given in Table 2. The requirement for Eq. 40 to be valid ($\kappa x > 0.2$) was satisfied under the experimental conditions employed in this work.

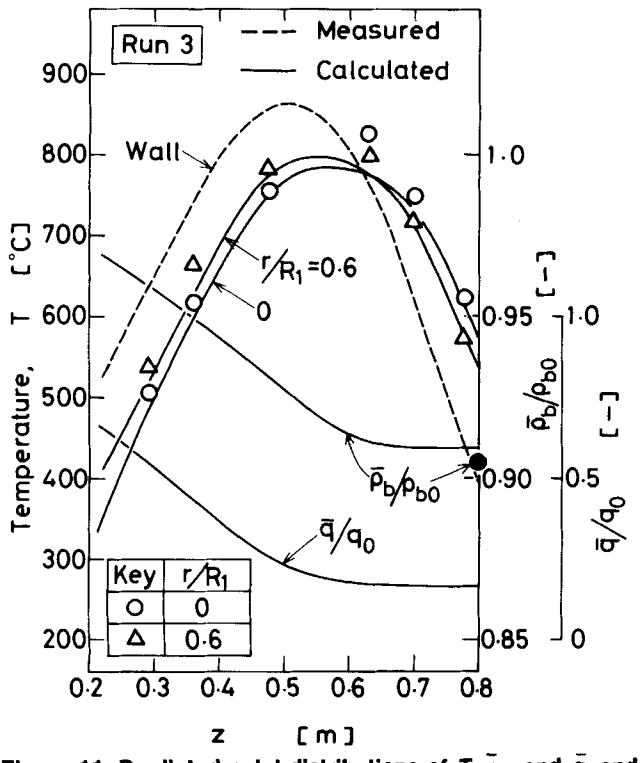

Figure 11. Predicted axial distributions of T, $\bar{\rho}_b$, and $\bar{q}$, and experimental data (run 3).

Figure 8 shows a comparison of the temperature distributions calculated by use of the determined k_e and h_w and the experimental data. The good agreement indicates that k_e and h_w were correctly estimated.

Distribution of Weight Loss and Temperature in the Moving-Bed Regenerator

Spent activated carbon was regenerated under four sets of experimental conditions, which are given in Table 3. The temperature distribution in the moving bed was measured in detail. The packed density of the regenerated carbon was also measured. Its value relative to that of the spent carbon ρ_b/ρ_{b0}, which is listed for each run in the table, corresponds to G_s/G_{s0} at the exit of the moving bed, because the particle diameter changes little during regeneration, as shown later.

The distributions of temperature, relative weight of spent carbon ρ_b/ρ_{b0}, and relative amount of residual adsorbate q/q_0, were calculated for each of the experimental conditions by use of the rate data for thermal regeneration and k_e and h_w obtained in the previous sections.

The heat of gasification, ΔH_C, was equated to 7,500 kJ/kg by assuming that the overall gasification reaction is represented by

$$C + 2H_2O \rightarrow CO_2 + 2H_2 \qquad (42)$$

The heat of pyrolysis, ΔH_P, was not measured but was taken to be 420 kJ/kg based on the work of Suzuki et al. (1978). They evaluated the heats of adsorption of 13 organic substances on an activated carbon at 38 to 146 kcal/kg. Therefore, ΔH_P was assumed to be 100 kcal/kg = 420 kJ/kg.

The effect of the ratio s^*/v^* on the calculated results was examined beforehand. No significant difference was found between calculated results even when the ratio was changed from 0

TABLE 4. CHANGES IN THE PHYSICAL PROPERTIES OF CARBON THROUGH REGENERATION

Sample	ρ_b kg/m³	ρ_p kg/m³	ρ_t kg/m³	$d_p \times 10^3$ m	$S_{BET} \times 10^{-5}$ m²/kg
Virgin	451	812	1,730	1.58	9.61
Spent	465	751	—	1.45	6.38
Regenerated					
Run 1	432	719	1,650	1.46	8.11
Run 2	422	712	1,620	1.44	8.12
Run 3	421	689	—	—	8.17
Run 4	435	691	1,690	1.42	8.52

to 0.5. This is because the gasification rate was very small under the experimental conditions employed in this work. The ratio s^*/v^* for such organic substances as sucrose (Chihara et al., 1981), dodecylbenzenesulfonate (Hashimoto et al., 1982) and *p*-nitrophenol are around 0.1 to 0.4. The ratio for *p*-nitrophenol was determined in this work by measuring the TG curve of an activated carbon on which it was adsorbed. The ratio was assumed to be 0.25 for the calculation in this work, though the calculated results vary little when the ratio lies between 0 and 0.5.

Figures 9a and 10a show the radial temperature distributions for runs 1 and 2, respectively. Figures 9b, 10b, 11 and 12 show the axial distributions of temperature, relative weight of spent carbon ρ_b/ρ_{b0}, and relative amount of residual adsorbate q/q_0, for all runs. The values of ρ_b and q were obtained by averaging ρ_b and q over the radial direction in the regenerator. In these figures the broken lines show the wall temperature distributions, which were regulated by five temperature controllers. In each run fairly good agreement was obtained between the calculated and experimentally measured temperature distributions. The slight discrepancies where the temperatures reached maxima are probably due to the neglect of evolved gases in developing the design equations. In each figure the calculated ρ_b/ρ_{b0} value at the outlet is also compared with the experimental value, which is shown by the closed circle. These values are also in fairly good agreement. These facts indicate that the temperature distribution in the moving bed and the weight loss of the regenerated carbon can be predicted well by the presented method.

Changes in Properties of Carbon Through Regeneration

Table 4 gives the packed density ρ_b, the particle density ρ_p, the true density ρ_t, the particle diameter d_p, and the pore surface area

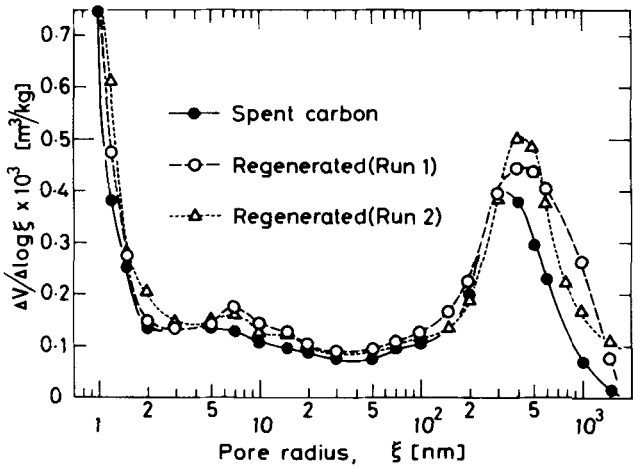

Figure 13. Pore volume distribution curves for spent and regenerated carbons.

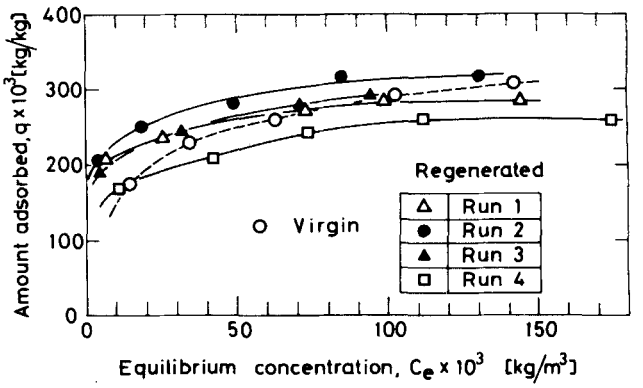

Figure 14. Adsorption isotherms of aqueous p-nitrophenol solution on virgin and regenerated carbons.

S_{BET} of the virgin, the spent, and the regenerated carbons. Since the spent activated carbon had been repeatedly used and regenerated, it differed greatly in such properties as particle density and particle diameter from the virgin carbon. This renders comparisons of the physical properties of the virgin and regenerated carbons meaningless. Therefore the spent and regenerated carbons were compared. The packed density and the particle density decreased through regeneration, whereas the particle diameter was almost unchanged. This seems to indicate that the adsorbed substances are preferentially removed through regeneration. The pore surface area increased considerably during regeneration.

Figure 13 shows the pore volume distribution curves for spent and regenerated carbons (runs 1, 2). It demonstrates that the pore volume is restored over the whole range of pore radii by the regenerating method employed in this work.

Finally, the adsorption isotherms of aqueous *p*-nitrophenol solution on the virgin and regenerated carbons were measured. The results are given in Figure 14. In all but run 4, the adsorption capacity of regenerated carbon is comparable to or greater than that of the virgin carbon.

These findings indicate that the regenerating method effectively removes the adsorbed substances without changing the particle diameter, and restores the adsorption capacity.

ACKNOWLEDGMENT

This research was supported by the Ministry of Education of Japan through a Grant-in-Aid for Scientific Research (Grant No. 555383).

NOTATION

C_e = equilibrium concentration of *p*-nitrophenol, kg/m³
$\bar{c}_p$ = averaged specific heat defined by Eq. 29, J/kg·K
$\bar{c}_{pg}$ = averaged specific heat of gas, J/kg·K
c_{ps} = specific heat of solid, J/kg·K
d_p = particle diameter, m
E = activation energy, J/mol, kJ/mol
$f(E)$ = distribution curve of activation energy, mol/J, mol/kJ
G = mass velocity defined by Eq. 29, kg/m²·h, kg/m²·s
G_g = mass velocity of gas, kg/m²·h, kg/m²·s
G_s = mass velocity of solid, kg/m²·h, kg/m²·s
h = dimensionless parameter defined by Eq. 37
h_w = wall heat transfer coefficient, W/m²·K
K = dimensionless term defined by Eq. 41

k_e = effective radial thermal conductivity, W/m·K
k_0 = frequency factor, s^{-1}
q = amount of residual adsorbate per initial unit weight of active carbon, kg/kg
$\bar{q}$ = q value averaged over radial direction in the moving-bed regenerator, kg/kg
R = gas constant, 8.314 J/mol·K
R_1 = inner radius of the moving-bed regenerator, m
R_2 = outer radius of the moving-bed regenerator, m
r = radial position in the moving bed, m
r_G = overall rate of gasification per unit weight of sample, kg/kg·s
r_P = overall rate of pyrolysis per unit weight of sample, kg/kg·s
r_T = overall rate of weight decrease per unit weight of sample, kg/kg·s
S_{BET} = pore surface area of active carbon, m^2/kg
s = weight of the carbonized adsorbate per initial unit weight of active carbon, kg/kg
s^* = s value at the completion of carbonization, kg/kg
T = temperature, K, °C
T_s = temperature at outer wall, K, °C
T_w = temperature at inner wall, K, °C
t = time, s, h
u_s = linear velocity of solid, m/s, m/h
V = pore volume of active carbon, m^3/kg
v = weight of volatile matter per initial unit weight of active carbon, kg/kg
v^* = weight of volatile matter evolved at the completion of pyrolysis, kg/kg
W_A = weight of active carbon, kg
W_T = total weight of sample, kg
z = axial position in the moving bed (measured from the top of the furnace), m

Greek Letters

α = constant in Eq. 12, s^{-1}
β = constant in Eq. 13, mol/J, mol/kJ
ΔH_G = heat of reaction of the gasification reaction per 1 kg of carbon gasified, J/kg, kJ/kg
ΔH_P = heat of reaction of the pyrolysis reaction to form 1 kg of volatile matter, J/kg, kJ/kg
κ = dimensionless parameter defined by Eq. 37
λ = thermal conductivity in the wall of the moving bed regenerator, W/m·K
ξ = pore radius of active carbon, nm
ρ_b = bulk density of bed, kg/m^3
$\bar{\rho}_b$ = ρ_b value averaged over radial direction in the moving-bed regenerator, kg/m^3
ρ_p = particle density, kg/m^3
ρ_t = true density of the particle, kg/m^3
ϕ_j = stoichiometric coefficient of the pyrolysis reaction
ψ_j = stoichiometric coefficient of the pyrolysis reaction

Subscripts

j = jth species of adsorbed substances
g = gasification
0 = initial value, value at the entrance of the moving bed

APPENDIX: METHOD OF SOLVING DESIGN EQUATIONS

To convert Eqs. 26–33 into finite difference equations, the indexes and increments in the radial and the axial directions in the moving-bed regenerator were chosen as follows:

1. Radial direction: The index was represented by $m = 0,1,2,\ldots,M$. Here $M = 20$, namely $\Delta r = 0.00235$ m.
2. Axial direction: The index was $n = 0,1,2,\ldots$ and the increment Δz was chosen as 0.008 m.

Equation 28 was approximated by the following equation at $m = m$ and $n = n + 1/2$.

$$-(G\bar{c}_p)_{av}\left.\frac{\partial T}{\partial z}\right|_{m,n+\frac{1}{2}} + k_e\left(\frac{\partial^2 T}{\partial r^2} + \frac{1}{r}\frac{\partial T}{\partial r}\right)_{m,n+\frac{1}{2}} + \delta_{av} = 0 \quad \text{(A1)}$$

where the subscript av indicates the averaged value between n and $(n+1)$th levels and the term δ_{av} was equated to

$$\delta_{av} = \frac{v^*}{q_0} G_{A0}\left(-\frac{\partial q}{\partial z}\right)_{av}(-\Delta H_P) + \frac{k_{0g}}{u_s} e^{-E_g/RT_{av}}[(G_A)_{av} + G_{A0}s_{av}] \quad \text{(A2)}$$

By applying the Crank-Nicolson implicit formula, Eqs. A1, 31, and 32 were reduced to finite-difference equations as

$$-(2+\gamma_{av})T_{0,n+1} + 2T_{1,n+1} = (2-\gamma_{av})T_{0,n} - 2T_{1,n} - \gamma_{av}\frac{\Delta z}{(G\bar{c}_p)_{av}}\delta_{av} = 0 \quad \text{(A3)}$$

$$\frac{1}{2}\left(1-\frac{1}{2m}\right)T_{m-1,n+1} - (1+\gamma_{av})T_{m,n+1} + \frac{1}{2}\left(1+\frac{1}{2m}\right)T_{m+1,n+1} = \frac{1}{2}\left(1-\frac{1}{2m}\right)T_{m-1,n} + (1-\gamma_{av})T_{m,n} - \frac{1}{2}\left(1+\frac{1}{2m}\right)T_{m+1,n} - \gamma_{av}\frac{\Delta z}{(G\bar{c}_p)_{av}}\delta_{av} = 0 \quad (m = 1,2,\ldots,M-1) \quad \text{(A4)}$$

$$T_{M-1,n+1} - \left[1+\gamma+\frac{1+\frac{1}{2M}}{B_0(A_0+1)}\right]T_{m,n+1} = -T_{M-1,n} + \left[1-\gamma+\frac{1+\frac{1}{2M}}{B_0(A_0+1)}\right]T_{M,n} - \frac{1+\frac{1}{2M}}{B_0(A_0+1)}(T_{s,n+1}+T_{s,n}) - \gamma_{av}\frac{\Delta z}{(G\bar{c}_p)_{av}}\delta_{av} \quad \text{(A5)}$$

where

$$\gamma_{av} = \frac{(G\bar{c}_p)_{av}(\Delta r)^2}{k_e \Delta z} \quad \text{(A6)}$$

$$A_0 = \frac{h_w R_1}{\lambda}\ln\frac{R_2}{R_1} \quad \text{(A7)}$$

$$B_0 = \frac{k_e}{\Delta r h_w} \quad \text{(A8)}$$

The terms $(-\partial q/\partial z)_{av}$, $(G_A)_{av}$, and s_{av} in δ_{av} were represented by

$$\left(-\frac{\partial q}{\partial z}\right)_{av} = \frac{q_0}{2u_s}\int_0^\infty k_0 e^{-E/RT_{av}}[\Phi_{m,n}(E) + \Phi_{m,n+1}(E)]f(E)dE \quad \text{(A9)}$$

$$(G_A)_{av} = G_{A0} \exp\left[-\frac{1}{2}(\chi_{m,n} + \chi_{m,n+1})\right] \quad \text{(A10)}$$

$$s_{av} = \frac{1}{2}(s_{m,n} + s_{m,n+1}) \quad \text{(A11)}$$

where

$$\Phi_{m,n}(E) = \exp\left(-\frac{k_0}{u_s}\int_0^z e^{-E/RT}dz\right) \quad \text{(A12)}$$

$$\chi_{m,n} = \frac{k_{0g}}{u_s}\int_0^z e^{-E_g/RT}dz \quad \text{(A13)}$$

$$s_{m,n} = \frac{s^*}{q_0}\exp(-\chi_{m,n})\psi_{m,n} \quad \text{(A14)}$$

$$\psi_{m,n} = \int_0^z \exp[\chi(r,z)]\left(-\frac{\partial q}{\partial z}\right)dz \quad \text{(A15)}$$

The values of $\Phi(E)$, χ, s, and ψ at $n = n + 1$ were calculated by

$$\Phi_{m,n+1}(E) = \Phi_{m,n}(E)\exp\left(-\frac{k_0}{u_s}e^{-E/RT_{av}}\Delta z\right) \quad \text{(A16)}$$

$$\chi_{m,n+1} = \chi_{m,n} + \frac{k_{0g}}{u_s}e^{-E_g/RT_{av}}\Delta z \quad \text{(A17)}$$

$$s_{m,n+1} = \frac{s^*}{q_0}\exp(-\chi_{m,n+1})\psi_{m,n+1} \quad \text{(A18)}$$

$$\psi_{m,n+1} = \psi_{m,n} + \exp\left[\frac{1}{2}(\chi_{m,n} + \chi_{m,n+1})\right]\left(-\frac{\partial q}{\partial z}\right)_{av}\Delta z \quad \text{(A19)}$$

By using Eqs. A9 to A19 the terms $(-\partial q/\partial z)_{av}$, $(G_A)_{av}$, and s_{av} can be calculated when T_{av} and the value of each term at n level are known. The values of q and G_s at the $n + 1$ level can be calculated from

$$q_{m,n+1} = q_{m,n} + \left(\frac{\partial q}{\partial z}\right)_{av}\Delta z \quad \text{(A20)}$$

$$(G_s)_{m,n+1} = (G_A)_{m,n+1} + G_{A0}(s_{m,n+1} + q_{m,n+1}) \quad \text{(A21)}$$

The procedure for solving these equations can be summarized as follows.

1. Assume $T_{m,n+1}$ equals $T_{m,n}$.
2. Calculate T_{av} by $T_{av} = (T_{m,n} + T_{m,n+1})/2$.
3. Calculate δ_{av} through Eqs. A2 and A9 to A19.
4. Calculate $(G\bar{c}_p)_{av}$ by use of Eqs. 29 and A21.
5. Equations A3 to A5 constitute a tridiagonal form of simultaneous linear equations of dimension $M + 1$. These equations can be solved to obtain $T_{m,n+1}(m = 0, 1, \ldots, M)$ by an appropriate method. Here, the so-called Thomas method was employed.
6. Repeat steps 2 to 5 by use of the determined $T_{m,n+1}$ until $T_{m,n+1}$ converges within allowable error.
7. Continue steps 1 to 6 until the exit of the moving bed.

LITERATURE CITED

Carslaw, H. S., and J. C. Jaeger, *Conduction of Heat in Solids*, Oxford Univ. Press, 193 (1959).

Chihara, K., J. M. Smith, and M. Suzuki, "Regeneration of Powdered Activated Carbon," *AIChE J.*, **27**, 213 (1981).

Hashimoto, K., K. Miura, and T. Watanabe, "Kinetics of Thermal Regeneration Reaction of Activated Carbons used in Waste-Water Treatment," *AIChE J.*, **28**, 737 (1982).

Loven, A. W., "Perspectives on Carbon Regeneration," *Chem. Eng. Prog.*, **69**, (11), 56 (1973).

Suzuki, M., et al., "Study of Thermal Regeneration of Spent Activated Carbons: Thermogravimetric Measurement of Various Single Component Organics Loaded on Activated Carbons," *Chem. Eng. Sci.*, **33**, 271 (1978).

Manuscript received June 21, 1984, and revision received Dec. 11, 1984.